UDC 551.526.6:551.507.362.2:535-1(261.6)

DETAILED SEA-SURFACE TEMPERATURE ANALYSIS UTILIZING NIMBUS HRIR DATA

FRED M. VUKOVICH

Research Triangle Institute, Research Triangle Park, N.C.

ABSTRACT

A technique that reduces the effect of noise in the Nimbus High Resolution Infrared Radiometer (HRIR) data and that yields sea-surface temperatures free of cloud interference has been developed. It allows a spatial resolution of about 20 n.mi. and the resulting HRIR temperature pattern compares well with ground truth data. A 1.0°C discrepancy was found between the modified HRIR data and the ground truth wherein the HRIR temperatures were lower than the ground truth values. HRIR data were corrected for attenuation by water vapor and carbon dioxide absorption.

1. INTRODUCTION

The advent of satellite-borne radiometric systems has introduced the prospect of studying sea-surface temperature patterns on a time and space scale unattainable by conventional means. Some of the earlier satellites, however, had radiometers with spatial resolutions too low to depict these patterns precisely. It was not until the High Resolution Infrared Radiometer (HRIR) was developed that the distortion produced by the radiometer resolution was reduced to an acceptable level. This radiometer was an integral part of the early Nimbus satellites (i.e., Nimbus 1, 2, and 3).

The HRIR data from these satellites, however, were afflicted with system noise. System noise is random or periodic signals produced by the total HRIR electronic system (tape recorder, telemetry system, etc.) and superimposed on the true radiative signature of an underlying surface. The Nimbus HRIR data had a large amplitude 200-Hz component and a small amplitude 100-Hz component (Fujita and Bandeen 1965, Williamson 1968). The noise in the HRIR data made detailed sea-surface temperature analysis extremely difficult (Vukovich and Blanton 1969, Krishna Rao 1968).

The necessity of removing noise is evident, but equally important is the necessity of attaining a sea-surface temperature analysis free of cloud effects. Under overcast conditions, it is impossible to obtain HRIR surface temperatures; but, in the case of scattered clouds, holes large enough to yield an unobstructed view of the surface may exist and allow HRIR measurement of the surface temperature. The problem then becomes a matter of discriminating between the cloud-contaminated temperature and the clear-sky temperature. A technique that both removes the predominant noise effects and establishes a temperature free of cloud effects in the Nimbus HRIR data is described below.

2. PROCEDURE

HRIR temperatures in a 20 n.mi. by 20 n.mi. area were constrained to fall within a range representative of temperatures expected under clear-sky conditions for the specific region and time of year. The range was based on mean monthly sea-surface temperature data corrected for atmospheric attenuation and the average effects of the noise. The average temperature correction for the geographic region, due to attenuation by water vapor and carbon dioxide in wavelength bands of the HRIR (Smith et al. 1970), was used to reduce the upper and lower bounds of the temperature range. The magnitude of the average error due to system noise was used to increase the upper bound and decrease the lower bound. The average error due to noise was assumed to be 2.0°C, which was derived from the Nimbus 2 HRIR noise analyses by Williamson (1968).

The temperatures selected in the 20 n.mi. square area under the prescribed constraints were averaged, and the average temperature represented the clear-sky temperature for the area. An average value was computed provided 50 percent of the temperatures in the given area fell within the effective clear sky range. Averaging over the 20 n.mi. by 20 n.mi. area would reduce the amplitude of the 200-Hz noise component, which has a wavelength on the surface of the earth of about 17–26 n.mi. depending on the height of the satellite and the angle of view. The average temperatures would reflect a near 100-Hz periodicity about the true signal.

The 100-Hz noise component would produce an oscillation in the surface temperature distribution having an effective wavelength of approximately 40–60 n.mi. depending on the satellite's altitude and the nadir angle. Averaging seven consecutive average temperatures along a line parallel to the scanline track would reduce the 100-Hz noise where each point was 10 n.mi. from the next because areas overlapped. This technique is similar to the technique used by Fujita and Bandeen (1965). However, averaging in this manner not only minimizes the noise but also reduces the resolution in the data. Data resolution can be maintained at a reasonable level while reducing the noise by making use of the fact that temperatures become uncorrelated rapidly in time and space. This requires that the data used in the averaging process be weighted

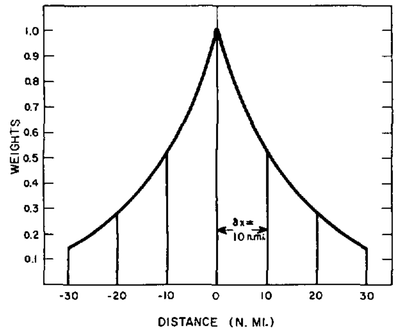

FIGURE 1.—Spatial variation of the weighting function for the 7-point weighted-running-mean technique.

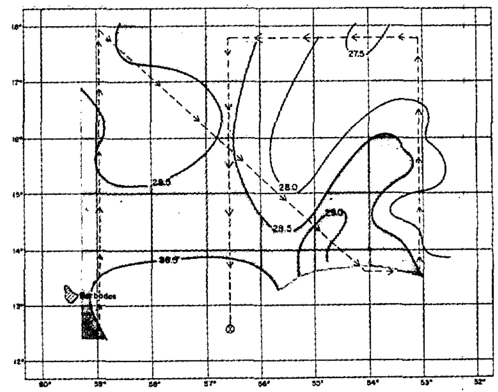

FIGURE 2.—Sea-surface temperature analysis (°C) in the BOMEX grid. These data were obtained by the R/V *Advance II* during Phase III of BOMEX and were intregrated over that period for the analysis. Dashed line indicates the cruise track of the ship during the period.

according to the relationship between data points, with the central point having the largest weight and those farthest away from the central point having the least weight.

For the analysis, the weighting factors were assumed to decay exponentially with distance from the central point. The rate constant was determined by trial and error, where ground truth data were employed as a basis to determine the accuracy of the results. The spatial characteristics of the weighting function for the "7-point weighted-running-mean technique", which yielded HRIR data that correlated best with ground truth data, are shown in figure 1. Equation (1) is the mathematical expression of the 7-point weighted-running-mean technique for a two-dimensional grid with m rows parallel to the scanline track and n columns perpendicular to the rows:

$$\begin{aligned}\overline{T}(n,m) = [&0.150\ T(n,m-3) + 0.284\ T(n,m-2)\\ &+ 0.533\ T(n,m-1) + T(n,m)\\ &+ 0.533\ T(n,m+1) + 0.284\ T(n,m+2)\\ &+ 0.150\ T(n,m+3)]\ (2.934)^{-1}. \qquad (1)\end{aligned}$$

Equation (1) can be used if seven consecutive points are available. Computations using six consecutive points were allowed in some cases provided the missing point, which resulted from the inability to determine a cloud-free temperature at the grid point, was not (n,m), $(n,m-1)$, or $(n,m+1)$. In these cases, the denominator in eq (1) was corrected for the missing point. In some cases, extreme cloudiness prevented the determination of cloud-free temperatures over an area. After the data were processed, temperatures were interpolated subjectively in these areas provided the area was small compared to the overall area of the analysis, and that sufficient peripheral data were available.

3. TEMPERATURE PATTERN STUDY (BOMEX DATA)

During Phase III of the Barbados Oceanographic and Meteorological Experiment (BOMEX, June 19 to July 2, 1969), the Research Triangle Institute, in conjunction with the Cape Fear Technical Institute, N.C., collected sea-surface temperature data over the entire BOMEX grid using the ship R/V *Advance II*. A thermistor probe was towed at the surface and a boom was used to keep the probe away from the wake of the ship. The sea-surface temperature data were integrated to give isotherms over the grid (fig. 2). In the analysis, temperatures greater than 28.5°C were shaded gray.

There is very little horizontal variability of the surface temperature in this region. The maximum temperature difference is 1.5°C. There is a warm water tongue oriented SW–NE just east of 56°W, and a cold tongue, also oriented SW–NE, north and west of the center of the warm tongue. These features also are evident in the mean sea-surface temperature analyses for June and July (Mazeika 1968). The region west of these features is characterized by a relatively small temperature variation.

Cloudiness prevented the attainment of Nimbus 3 HRIR data for the entire Phase III grid during the integration period. It was not until July 11, 1969, that the sky was sufficiently clear to allow coverage of the sea surface over the entire area.

The unsmoothed Nimbus 3 HRIR data are shown in figure 3. An isotherm interval of 4°C was employed to minimize the effect of noise and scattered clouds. Areas with temperatures greater than 23°C were shaded. No attempt was made to correct the HRIR temperatures for atmospheric attenuation in this or subsequent analyses. Discussion of temperature magnitudes is given in section 5.

A large area of low temperatures is shown in the southwest quadrant. These temperatures are too low to be associated with sea-surface radiation or known effects of system noise, and apparently are related to radiation from clouds. Other relative cold areas also are present north of that area, and these too are most probably produced by clouds. The remaining areas were presumed either free of clouds or under the influence of scattered clouds.

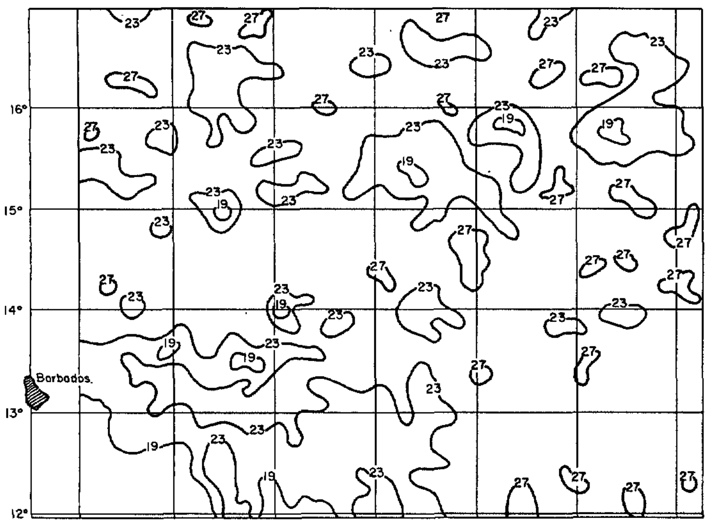

FIGURE 3.—Sea-surface temperature analysis (°C) on the BOMEX grid for July 11, 1969, using unsmoothed Nimbus 3 HRIR data.

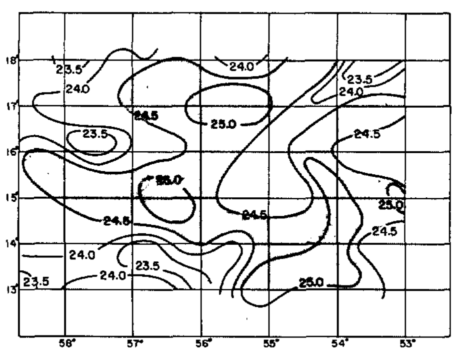

FIGURE 4.—Sea-surface temperature analysis (°C) on the BOMEX grid for July 11, 1969, using Nimbus 3 HRIR data smoothed by the 7-point weighted-running-mean technique.

Figure 4 shows the same HRIR data filtered by the 7-point weighted-running-mean technique. The clear-sky temperature range used was 23°–27°C—determined by using the mean temperatures for July and the *Advance II* data. Areas with temperatures greater than 24.5°C are shaded gray.

The eastern portion of the grid shows the juxtaposition of cold and warm water tongues that was found in the ground truth data (fig. 2). The orientation of the cold tongue and portions of the warm tongue is SW–NE. The maximum temperature difference between the warm and cold tongue is 2.2°C, which compares reasonably well with the ground truth value (1.5°C). In the satellite data, these features are shifted about 0.5° to the east of their observed position.

The western portion of the grid shows two relative cold areas separated by a relative warm zone stretching east and west. This is similar to the pattern observed in the *Advance II* data. The temperature variations, however, are more pronounced than indicated in the ground truth

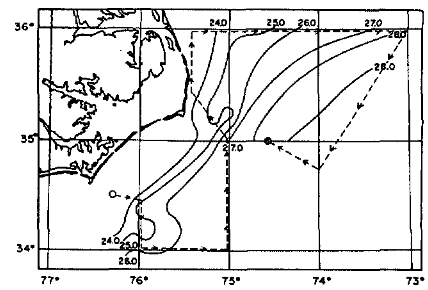

FIGURE 5.—Sea-surface temperature analysis (°C) off the North Carolina coast. The data were obtained by the R/V *Eastward* and were integrated over the period July 21–30, 1966. Dashed line indicates the cruise track of the ship during the period.

analysis. The maximum temperature difference in that area is about 1.5°C and the average difference is 1.0°C. The ground truth data indicated that the maximum temperature difference is 0.8°C. It appears that this pattern is displaced northward less than 0.5°.

The position discrepancies could be due to real displacements of the pattern since there is a 15-day time lag between measurements. However, the displacement indicated is about 40 n.mi. to the northeast; whereas mean surface currents in that area (Schott 1944) would produce a westward displacement. This suggests that the position discrepancy was not due to real displacements.

The satellite data are known to have an inherent position error. In other studies, known landmarks have been used to attain accurate registration for the satellite data; however, this is not possible over the open sea. This problem must be resolved in order to establish real variations. Shifting the satellite data 40 n.mi. southwestward would result in a better correlation in this case.

4. TEMPERATURE PATTERN STUDY (GULFSTREAM DATA)

Nimbus 2 HRIR data were compared with sea-surface temperature data obtained by the Duke University Marine Laboratory's ship R/V *Eastward* off the North Carolina coast. The *Eastward* sea-surface temperatures were measured by the same technique described in section 3. For this case, data were integrated over the 9-day period July 21–30, 1966. Figure 5 shows the *Eastward* data analysis.

The analysis shows cold water just off the North Carolina coast (temperatures less than 24°C) and the warm water characteristic of the Gulf Stream (temperatures in excess of 28°C). The inner edge of the Gulf Stream is found 36 n.mi. east of Cape Lookout and 15 n.mi. east of Cape Hatteras. The boundary is oriented NE–SW. East of Cape Hatteras there are alternating warm and cold water tongues and a cold tongue is found southeast of Cape Lookout.

A detailed examination of the unfiltered Nimbus 2 HRIR data (fig. 6), which are extremely noisy, revealed a

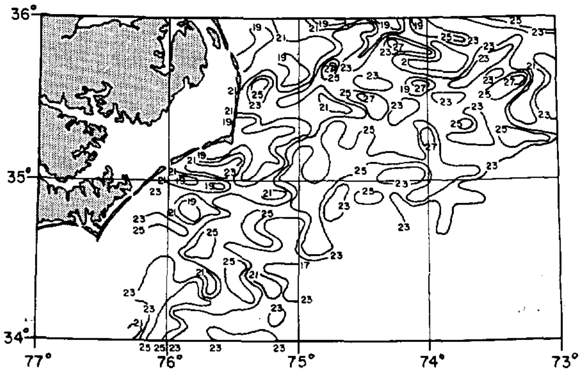

FIGURE 6.—Sea-surface temperature analysis (°C) off the North Carolina coast for July 27, 1966, using unsmoothed Nimbus 2 HRIR data.

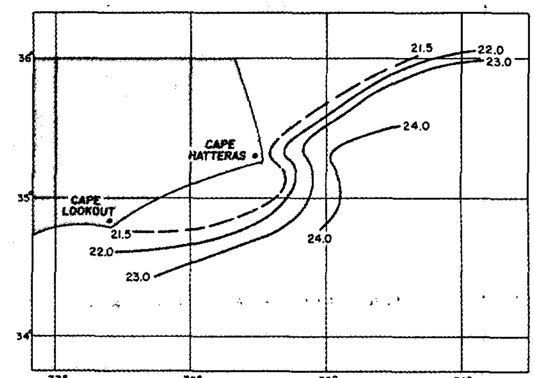

FIGURE 7.—Sea-surface temperature analysis (°C) off the North Carolina coast for July 27, 1966, using Nimbus 2 HRIR data smoothed by the 7-point weighted-running-mean technique.

series of warm water pockets oriented NE–SW that might be interpreted as the Gulf Stream. Cooler water is found adjacent to the coast. The location of the Gulf Stream's inner edge is obscure because of the lack of the continuous temperature field which normally characterizes the Gulf Stream. There are indications east and north of Cape Hatteras of the alternating warm and cold tongues found in the ground truth data, but these features appear further north in the HRIR analysis. The HRIR data were positioned by alining the pattern of equivalent blackbody temperatures at the North Carolina coast with the coastal geometry. The discrepancy between the location of the alternating cold and warm water tongues in the HRIR data and in the ground truth data is either a real-time variation, or is produced by noise and clouds. The HRIR data produced some enlighting aspects of this feature.

In the application of the 7-point weighted-running-mean technique in this case, an effective clear-sky range of 20°–27°C was used, derived from mean monthly data (Selfridge et al. 1968). The filtered HRIR data (fig. 7) show a distinct similarity to the ground truth pattern. The temperature field is continuous—unlike the unsmoothed data. The inner edge of the Gulf Stream is located approximately 40 n.mi. east of Cape Lookout and 15 n.mi. east of Cape Hatteras and is oriented NE–SW. Indications of the alternating warm and cold water tongues in the approximate position determined by the ground truth analysis are shown but the pattern is not as pronounced. It must be noted that the analytical technique produces a data void from the coast to a point 20 n.mi. east southeast. The temperatures in this area were extrapolated. The existing data contained enough of the pattern to render sufficient confidence in the results. Cloudiness obscured the sea surface in the southern regions so that clear-sky temperatures could not be determined.

Figure 8 presents the temperature profile along the 35.3°N latitude line from Cape Hatteras eastward. According to the *Eastward* data, the temperature change in the first 20 n.mi. is of the order of 1.1°C, and that found from the HRIR data is 1.5°C. In the next 10 n.mi., the

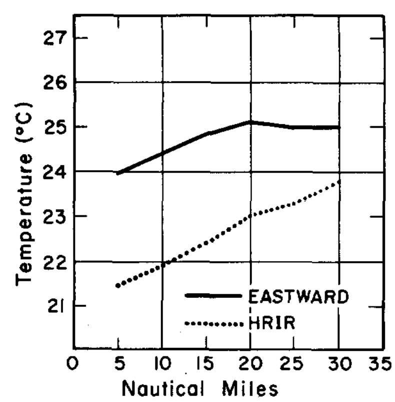

FIGURE 8.—Ship R/V *Eastward* and smoothed HRIR temperature (°C) profiles from the North Carolina coast eastward along the 35.3°N latitude line.

Eastward data show small negative temperature changes. The HRIR data show a continual increase in temperature, but at a decreasing rate. This is the region of the alternating warm and cold tongues which is more dramatically portrayed in the *Eastward* data than in the HRIR data. The differences might be real; that is, the differences might reflect discrepancies that would result normally in the comparison of instantaneous data with averaged data. However, they might be due to the smoothing produced by the filtering technique, or a combination of both factors.

5. MAGNITUDE STUDY

The magnitude discrepancies between the ground truth data and the Nimbus HRIR data observed in the previous section were attributed, in the first approximation, to the effects of the intervening atmosphere. Specifically, there is a radiation loss due to absorption by water vapor and carbon dioxide. These gases have been determined to be the major absorbers in the wavelength band of the HRIR. The absorption results in lower equivalent blackbody temperatures. To determine the accuracy of the technique, we must evaluate the effects of this absorption. The

446-553 O - 71 - 2

TABLE 1.—*Tabulation of the equivalent blackbody temperature, T_c, acquired through solution of the radiative transfer equation; of the HRIR temperature filtered by the 7-point weighted-running-mean technique, T_{7-pt}; and the difference between T_c and T_{7-pt} ($\Delta T = T_c - T_{7-pt}$). The latitudes and longitudes give the position of the HRIR data.*

Date	Latitude (°N)	Longitude (°W)	T_c (°C)	T_{7-pt} (°C)	ΔT (°C)
6/20/69	15	59	26.5	25.6	0.9
	13	59	26.5	24.1	2.4
6/26/69	15	56	26.4	25.3	1.1
	13	54	26.1	25.5	0.6
7/11/69	15	56	26.4	25.1	1.3
	13	54	26.1	24.9	1.2
7/22/69	15	56	26.5	24.6	1.9
7/27/66	35.3	75	24.2	23.5	0.7

magnitude of the HRIR temperature can be determined by either simulating the process through which radiation from the sea surface reaches the satellite, or by correcting the HRIR temperatures for the absorption loss. In this study, both procedures were used.

The technique used by Vukovich and Blanton (1969) to solve the radiative transfer equation was employed to simulate the radiative process. Source (sea surface) temperatures used for the calculations in the BOMEX array were obtained from the BOMEX Preliminary Data (BOMAP 1969). These temperatures were used instead of the *Advance II* data because of the time correlations between these and the HRIR data. Temperature observations were chosen from those ships with upper air soundings nearest to the selected HRIR observation. For the calculations made off the east coast of North Carolina, the *Eastward* data provided the source temperatures, and the upper air data were obtained from the Cape Hatteras radiosonde. The upper air data provided the pressure, temperature, and humidity data required for the computations. Carbon dioxide was assumed to be thoroughly mixed in the atmosphere with a mixing ratio of 0.5 g/kg and the emissivity of the sea surface was assumed to be 0.98 after Saunders and Wilkins (1967). The resulting computations gave the clear sky, equivalent blackbody temperatures, T_c. These were compared with HRIR temperatures. The results for a number of cases in the BOMEX array and for the July 1966 Gulf Stream case are given in table 1.

The table shows that in all cases T_c was greater than T_{7-pt}, the HRIR temperature obtained by filtering via the 7-point weighted-running-mean technique. The average temperature difference was 1.2°C, and the range was $0.6°\text{C} \leq \Delta T \leq 2.4°\text{C}$.

The second technique employed to assess the magnitude of the HRIR temperatures was to correct these temperatures for the atmospheric effects and compare them with the ground truth data. The corrections used were those determined by Smith et al. (1970). They were applied only to Nimbus data available in or near BOMEX Phase III

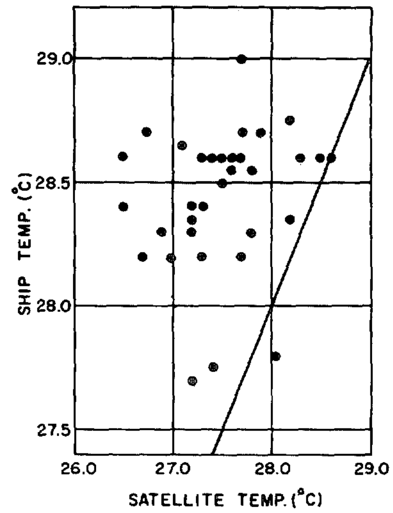

FIGURE 9.—Scattered diagram of ground truth data versus HRIR data smoothed by the 7-point weighted-running-mean technique.

and compared with the *Advance II* data. The results are depicted in the scatter diagram (fig. 9).

The sloping line in the figure is the line of perfect fit. The ship temperatures were higher than the satellite temperatures determined by the 7-point weighted-running-mean technique in all cases but two. In only one of the two exceptions was the satellite temperature higher than the ship temperature. In the other case, the two were equal. The average temperature difference between the ship's temperature, T_s, and the satellite temperature (temperature difference equals $T_s - T_{7-pt}$) was 1.0°C, which compares favorably with that found in the previous study.

The results of both comparisons indicate that the HRIR temperatures obtained through filtering via the 7-point weighted-running-mean technique are, on the average, a little more than 1.0°C lower than the ground truth temperatures. This discrepancy could be produced by extinction (absorption and/or scattering) of radiation by sea spray and aerosols (Noble et al. 1969, Vukovich and Blanton 1969) that was not accounted for in the solution of the radiative transfer equation. There is also the possibility that the temperature difference can be a result of the influence of some small cloud elements in the field of view of the radiometer that were not filtered.

6. SUMMARY AND CONCLUSIONS

This paper describes an analysis technique which minimized the effects of cloudiness and system noise in the Nimbus HRIR data while maintaining adequate resolution—approximately 20 n. mi. The noise abatement procedure was based on the premise that the major components characterizing the noise in the data were centered about two frequencies: (1) 100 Hz and (2) 200 Hz. Sufficient evidence existed to substantiate the premise. A filter was designed to minimize the noise at these frequencies. Filter design was based on the contention that the temperatures became rapidly uncorrelated in time (and, therefore, in space). The selection of HRIR temperatures free of cloud effects was performed by defining an effective clear-sky temperature range, and by choosing temperatures which fell within the range. The effective clear-sky temperature range was based on the sea-surface temperature statistics of the particular area and for the particular time of year, on the effects of gas-phase absorption of radiant energy, and on the average effects of the system noise.

The case studies indicated that considerable improvement in the HRIR sea-surface temperature pattern occurred when the data filtering technique was applied. The qualitative features of the temperature pattern (e.g., the position of the Gulf Stream's boundary and temperature oscillations such as warm water tongues) were reasonably evident. The magnitudes of the temperature gradients were approximately equivalent to gradients in ground truth data.

The filtered HRIR temperatures were, on the average, 1.0°C lower than ground truth temperatures after correcting for atmospheric attenuation. The difference can be attributed to the influence of small cloud elements that could not be filtered or to attenuation of radiation energy, through absorption or scattering by gases and particulate matter, unaccounted for in the correction.

ACKNOWLEDGMENTS

This research was sponsored by the National Environmental Satellite Service under Contract No. E-236-69(N). Dr. P. Krishna Rao was Contract Monitor. The author wishes to acknowledge the interest and the assistance of Mr. Howard Ruedger in developing the analysis techniques, and of Mr. Richard Haws, who did the computer programming. Special thanks to Mr. Thomas Cherrix, NASA, Goddard Space Flight Center, for his assistance with the Nimbus HRIR data.

REFERENCES

BOMAP, *BOMEX Preliminary Data: Volume I.—Ship Station Surface Observations; Volume II.—Ship Station Radiosonde Observations; Volume III.—Salinity-temperature-Depth Observations; Volume IV.—Sea-Surface Temperature Observations*, Barbados Oceanographic and Meteorological Analysis Project Office, ESSA, Rockville, Md., Dec. **1969**, 205, 443, 434, and 207 pp.

Fujita, Tetsuya, and Bandeen, William R., "Resolution of the Nimbus High Resolution Infrared Radiometer," *Journal of Applied Meteorology*, Vol. 4, No. 4, Aug. **1965**, pp. 492–503.

Krishna Rao, P., "Sea Surface Temperature Measurements From Satellites," *Mariners Weather Log*, Vol. 12, No. 5, Sept. **1968**, pp. 152–154.

Mazeika, Paul A., "Mean Monthly Sea-Surface Temperature and Zonal Anomalies of the Tropical Atlantic," *Serial Atlas of the Marine Environment*, Folio 16, American Geographical Society, New York, N.Y., **1968**, 9 pp.

Noble, V. E., Ketchum, R. D., and Ross, D. B., "Some Aspects of Remote Sensing as Applied to Oceanography," *Proceedings of the IEEE*, Vol. 57, No. 4, Apr. **1969**, pp. 594–604.

Saunders, Peter M., and Wilkins, Charles H., "Precise Airborne Radiation Thermometry," *Proceedings of the 4th Symposium on Remote Sensing of the Environment, Ann Arbor, Michigan, April* 1966, University of Michigan Press, Ann Arbor, June **1966**, pp. 815–826.

Schott, Gerhard, *Geographie des Atlantischen Ozeans* (Geography of the Atlantic Ocean), 3rd Edition, C. Boysen Co., Hamburg, Germany, **1944**, 438 pp.

Selfridge, S. W., Woodworth, W. C., and Richards, K. G., *Three-Dimensional Digital Ocean Climatology for the Western North Atlantic*, Litton Systems, Inc., Monterey, Calif., Feb. **1968**, numerous separately paginated sections.

Smith, W. L., Rao, P. K., Koffler, R., and Curtis, W. R., "The Determination of Sea-Surface Temperature From Satellite High Resolution Infrared Window Radiation Measurements," *Monthly Weather Review*, Vol. 98, No. 8, Aug. **1970**, pp. 604–611.

Vukovich, Fred M., and Blanton, Jackson O., "Physical Oceanography Feasibility Study Utilizing NIMBUS II HRIR Satellite Data," *Final Report*, ESSA Contract No. E-256-68(N), Research Triangle Institute, Research Triangle Park, N.C., July **1969**, 133 pp.

Williamson, E. J., "The Accuracy of the NIMBUS II High Resolution Infrared Radiometer," National Aeronautics and Space Administration, Greenbelt, Md., **1968**, 18 pp. (unpublished manuscript).

[Received December 21, 1970; revised May 13, 1971]